Biogeosciences Discuss., 10, 15519–15557, 2013
www.biogeosciences-discuss.net/10/15519/2013/
doi:10.5194/bgd-10-15519-2013

Biogeosciences Discussions
Open Access

Springtime phytoplankton dynamics in the Arctic Krossfjorden and Kongsfjorden (Spitsbergen) as a function of glacier proximity

A. M.-T. Piquet[1], W. H. van de Poll[2], R. J. W. Visser[1], C. Wiencke[3], H. Bolhuis[4], and A. G. J. Buma[1]

[1]Department of Ocean Ecosystems, Energy and Sustainability Research Institute Groningen, University of Groningen, Nijenborgh 7, 9747 AG Groningen, the Netherlands
[2]Department of Biological Oceanography, Royal Netherlands Institute for Sea Research, P.O. Box 59, 1790 AB Den Burg, Texel, the Netherlands
[3]Department of Functional Ecology, Alfred Wegener Institute, Am Handelshafen 12, 27570 Bremerhaven, Germany
[4]Marine Microbiology, Royal Netherlands Institute for Sea Research, P.O.Box 140, 4400 AC Yerseke, the Netherlands

Received: 22 August 2013 – Accepted: 30 August 2013 – Published: 1 October 2013

Correspondence to: A. M. T. Piquet (a.m.t.piquet@rug.nl)

Published by Copernicus Publications on behalf of the European Geosciences Union.

BGD
10, 15519–15557, 2013

Abstract

The hydrographic properties of the Kongsfjorden – Krossfjorden system (79° N, Spitsbergen) are affected by Atlantic water incursions as well as glacier meltwater runoff. This results in strong physical gradients (temperature, salinity and irradiance) within the fjords. Here, we tested the hypothesis that glaciers affect phytoplankton dynamics as early as the productive spring bloom period. During two campaigns in 2007 (late spring) and 2008 (early spring) we studied hydrographic characteristics and phytoplankton variability along 2 transects in both fjords, using HPLC-CHEMTAX pigment fingerprinting, molecular fingerprinting (DGGE) and sequencing of 18S rRNA genes. The sheltered inner fjord locations remained colder during spring as opposed to the outer locations. Vertical light attenuation coefficients increased from early spring onwards, at all locations, but in particular at the inner locations. During the end of spring, meltwater input had stratified surface waters throughout the fjords. The inner fjord locations were characterized by overall lower phytoplankton biomass. Furthermore HPLC-CHEMTAX data revealed that diatoms and *Phaeocystis* sp. were replaced by small nano- and picophytoplankton during late spring, coinciding with low nutrient availability. The innermost stations showed higher relative abundances of nano- and picophytoplankton throughout, notably of cyanophytes and cryptophytes. Molecular fingerprinting revealed a high similarity between inner fjord samples from early spring and late spring samples from all locations, while outer samples from early spring clustered separately. We conclude that glacier influence, mediated by early meltwater input, modifies phytoplankton biomass and composition already during the spring bloom period, in favor of low biomass and small cell size communities. This may affect higher trophic levels especially when regional warming further increases the period and volume of meltwater.

BGD
10, 15519–15557, 2013

1 Introduction

The Kongsfjorden (79° N, West Spitsbergen) is influenced by a highly variable inflow of Atlantic water from the West Spitsbergen Current (WSC) (Cottier et al., 2005; Hegseth and Tverberg, 2013), which transports relatively warm saline water ($T > 3$ °C and $S > 34.9$ psu) northwards (Hop et al., 2006; Schlichtholz and Goszczko, 2006; Svendsen et al., 2002). As a result, the fjords located on the western side of Spitsbergen are characterized by relatively mild temperatures, compared with other Arctic locations at similar latitude. Disrupted wintertime cooling of Arctic waters is expected to facilitate the WSC inflow into Kongsfjorden as well as in the Arctic at large (Buchholz et al., 2010). The Kongsfjorden and adjacent Krossfjorden are glacial fjords that are fed with freshwater by several large glaciers and streams (Cottier et al., 2005; Svendsen et al., 2002). Freshwater influx is highest in summer and co-occurs with a strong increase in sediment load, which can strongly limit light penetration (Keck et al., 1999; Svendsen et al., 2002).The meltwater discharge affects a large area in the fjord, up to 45 km distance from the glacier front and up to 30 m depth (Hop et al., 2002, 2006; Keck et al., 1999; Svendsen et al., 2002) and leads to strong surface stratification during summer. Due to enhanced WSC influence, the concomitant warming is expected to increase the magnitude and time interval of meltwater influx into the Kongsfjorden.The time window of meltwater discharge in the Kongsfjorden is not clearly described; in particular to what extent it affects water column characteristics during the spring months (April–June).

The observed hydrographic variability leads to a high level of unpredictability in interannual phytoplankton spring bloom timing, biomass and production. For example, enhanced inflow of warm Atlantic water in the Kongsfjorden is associated with changes in phytoplankton abundance and composition (Hegseth and Tverberg, 2013; Hodal et al., 2012): years with less inflow showed diatom dominance during the spring bloom whereas high inflow years were characterized by *Phaeocystis pouchetii* dominated spring blooms. Therefore, the timing, composition, and biomass of the spring bloom show extensive year to year variability (Hegseth and Tverberg, 2013). During summer

BGD
10, 15519–15557, 2013

stratification, diatoms and *P. pouchetii* become nutrient limited, are grazed upon or sink out of the euphotic zone. As a result, a transition occurs towards less productive, small sized, but highly diverse plankton communities (Hegseth and Sundfjord, 2008; Piquet et al., 2010). In addition to low nutrient availability, high sediment concentrations derived from glacial melt water input limit light availability for phytoplankton growth during summer. The euphotic zone can be restricted to the upper 0.3 m close to the glaciers (Keck et al., 1999) leading to highly unfavorable conditions for phytoplankton growth (Hop et al., 2006). Thus, the expected increase in magnitude of land derived meltwater influx may affect phytoplankton composition and production. In addition, when the onset of meltwater discharge would start earlier in the spring period (April–June), phytoplankton spring blooms may be affected, in particular at inner fjord locations. In the Western Antarctic Peninsula region, changes in phytoplankton composition and size were observed, related with regional warming (Moline et al., 2004; Montes-Hugo et al., 2009). A significant decrease in average phytoplankton cell size was associated with enhanced meltwater input, favoring nanophytoplankton, notably cryptophytes. Similar observations were made in the Pacific Arctic (Canada Basin and Chukchi Sea) where smaller sized phytoplankton species appeared to thrive under summertime surface freshening and impoverished sea ice conditions (Coupel et al., 2012; Li et al., 2009). Summertime freshening was associated with an increase in pico- and bacterioplankton abundance, while altered sea ice conditions caused a spatial shift in phytoplankton distribution as well as an increase in nanoplankton abundance.

Although extensive information exists on larger microalgal species occurring in the Kongsfjorden (Hasle and Heimdal, 1998; Hop et al., 2002; Keck et al., 1999), only a few studies described the taxonomic composition in the nano- and picophytoplankton size ranges (Rokkan Iversen and Seuthe, 2011). Molecular techniques offer an efficient, high-resolution approach to complement classical micro-eukaryotic community analyses. In 2005 we performed a study to investigate summer phytoplankton diversity and composition in Kongsfjorden and Krossfjorden, using a combination of molecular approaches (Piquet et al., 2010). During this study the Kongsfjorden and Krossfjor-

BGD
10, 15519–15557, 2013

den were found to harbor distinctive micro-eukaryotic communities during the stratified summer period. The results suggested that meltwater input during summer structured marine microbial communities through decreased salinity, increased light attenuation, and strong salinity stratification. However, nothing was known about the possible impact of meltwater discharge during spring and how this would affect timing, extent and composition of phytoplankton dynamics. With increasing global warming, an earlier discharge of fresh meltwater is a likely scenario and therefore information is required to be able to understand the consequences of enhanced glacial melting on phytoplankton performance, in particular during the season of highest productivity, e.g. April–June.

The aim of the present study was to analyze the dynamics and composition of springtime phytoplankton communities in response to prevailing water mass properties, glacier vicinity and meltwater release. We hypothesize that during the spring bloom period phytoplankton is already affected by glacial meltwater input, in particular at inshore locations. Phytoplankton variability was studied in two consecutive years, covering spring (2008) and early summer (2007), along a 3-station mini-transects in the Kongsfjorden and adjacent Krossfjorden. HPLC derived pigment fingerprinting followed by CHEMTAX calculation of taxon specific contributions to total phytoplankton biomass were related to physical and chemical environmental variables. In addition, molecular characterization of the eukaryotic community provided complementary information on community dynamics, diversity and composition by denaturing gradient gel electrophoresis (DGGE) of partial 18S rRNA genes and direct gene sequencing.

2 Materials and methods

2.1 Field sampling

Samples were collected in Kongsfjorden (78°57′54″ N and 11°51′24″ E) and Krossfjorden (79°10′00″ N 11°46′00″ E), located on the West coast of Spitsbergen in the Atlantic sector of Arctic Ocean. The five sampling sites were representative for ocean to glacier

BGD
10, 15519–15557, 2013

influenced locations within the fjords. The stations consisted of an "ocean" station (O) at the intersection of both fjords, a station in the middle (M, KM) and a station near the main glacier (G, KG) of each fjord (Fig. 1). Water samples were collected twice a week, provided weather conditions permitted boating activities, during two spring-summer field campaigns in 2007 and 2008. The 2007 campaign was conducted in late spring from 22 May to 25 June 2007, and in early spring of 2008 from 9 April to 12 May.

Standard sampling depths were 0 and 20 m. Surface samples were collected directly using clean 12 L polyethylene carboys. Deeper samples were collected with a 12 L Niskin bottle (General Oceanics, Inc. Miami, Florida, USA) mounted 2 m above a Sea-Bird CTD (SNE 19plus, Sea-Bird Electronics, Inc. Bellevue, Washington, USA). The CTD was fitted with a biospherical Li-Cor PAR (Photosynthetic Active Radiation) sensor (Sea-Bird Electronics), and in 2008 supplemented with a Wetstar fluorometer (Wet labs, Inc. Philomath, Oregon, USA). All samples were collected in the morning, stored cold and dark during transportation and processed within 3 h at the Kingsbay Marine Laboratory, Ny-Ålesund. Samples for inorganic nutrient analysis were processed immediately on board. For each sample, 5 mL filtrate was obtained by filtration over a sterile 0.2 µm pore size cellulose acetate syringe filter (Whatman GmbH, Dassel, Germany). Vials destined for silica analysis were kept at 4 °C, while vials for nitrate, nitrite, and phosphate analysis were stored at −80 °C until analysis on a an AxFlow Bran+Luebbe Traacs800 autoanalyzer at the Royal NIOZ laboratory (Texel, the Netherlands).

2.2 Sample processing

Upon return to the Kingsbay Marine Laboratory water samples were immediately filtered by vacuum pressure (maximum 0.5 bar). For pigment analysis, 6 liters of seawater were filtered onto 47 mm GF/F filters. The filters were snap frozen in liquid nitrogen and stored at −80 °C until analysis. For molecular analysis, we filtered 1.5 to 2 L of seawater onto 47 mm 2 µm pore size polycarbonate filters (Merck Millipore, Massachusetts, USA). The use of 0.2 µm polycarbonate filters, which might have been more appropriate to cover the full phytoplankton size spectrum, was not successful. This pore size

BGD
10, 15519–15557, 2013

caused early clogging of filters due to the presence of inorganic particles, and as a result restricted the filter volume but elongated filtration time beyond what was acceptable. Therefore we chose to use 2 µm filters, even though we were aware of (partly) losing < 2 µm picophytoplankton cells. Filters were stored at −80 °C, until further analysis in the home laboratory. For qualitative microscopy analysis, one liter of seawater was fixed with Lugol's iodine solution (1 % final concentration) supplemented with formaldehyde (2 % final concentration) and left to settle at 4 °C. After one week, samples were concentrated to 100–150 mL by careful siphoning of the supernatant. The concentrated samples were transferred to 150 mL brown glass bottles with a Teflon lined screw cap and kept in the dark at 4 °C until processing.

2.3 Pigment analysis

Filters were freeze-dried for 48 h and immediately extracted in 5 mL 90 % acetone (*v*/*v*, 48 h, 4 °C) in the dark. Pigments were quantified using High Performance Liquid Chromatography (HPLC). Pigment extracts were separated on a Waters 960 HPLC system using a C^{18} 5 µm DeltaPak reversed phase column (Waters). The different pigments were identified by retention time and diode array detection at 436 nm. We used pigment standards obtained from DHI LAB Products to calibrate the HPLC. The CHEMTAX 1.95 program (Mackey et al., 1996) was used to determine the taxonomic contribution of different phytoplankton groups. The program uses the steepest-descent algorithm to determine the best fit based on an estimate of pigment: chl *a* ratios for different algal classes (Mackey et al., 1996). We used an initial pigment-ratio matrix derived from a Southern Ocean data set, to compute our data. The pigments implemented in the CHEMTAX analysis were chl *c*3, 19'-butanoyloxyfucoxanthin, fucoxanthin, 19'-hexanoyloxyfucoxanthin, prasinoxanthin, peridinin, alloxanthin, violaxanthin, lutein, zeaxanthin, chl *a* and chl *b*. The analysis provides estimates on the relative contribution of dinoflagellates, cryptophytes, chlorophytes (chlorophytes and prasinophytes were not distinguished), diatoms, haptophytes (where haptophytes 6 and 8 were pooled) and cyanobacteria. From the CHEMTAX

BGD
10, 15519–15557, 2013

results the pico-nanophytoplankton fraction was calculated, which was for this study based on cyanobacteria+cryptophytes+chlorophytes only. We omitted the dinoflagellates and haptophytes in these calculations, because dinoflagellate diversity was high, consisting of athecate and thecate cells in both $\ll 20\,\mu m$ and $\ll 20\,\mu m$ size ranges (as revealed by microscopy). In addition, the colony form of *Phaeocystis* sp. ($\ll 20\,\mu m$) seemed to dominate the haptophyte community (based on microscopic inspection).

2.4 Microscopy analysis

A few samples (30) were selected for microscopy analysis, mainly for comparative purposes associated with the CHEMTAX and molecular fingerprinting outcomes. Microscopy samples were processed following the Untermöhl technique. 10–25 mL of fixed samples was left to settle for 48 h in counting chambers. Phytoplankton species composition was qualitatively assessed, along one or two meridians at 40 × and 200 × magnifications on an Olympus IMT-2 inverted microscope.

2.5 DNA extraction and amplification

For molecular fingerprinting and sequencing, genomic DNA was extracted under sterile conditions as described previously (Piquet et al., 2010). DNA amplification of the 18S rRNA gene was carried out with the universal eukaryotic primer set Euk1A and 516r (Díez et al., 2001). We also used Euk1a in combination with the GC-clamp enriched reverse primer (516r-GC), for denaturing gradient gel electrophoresis (DGGE). Approximately 10 ng of DNA was used as template in the polymerase chain reaction (PCR). 50 µL PCR reaction contained each primer at a concentration of 300 nM, as well as 0.2 mM dNTPs, 2 mM $MgCl_2$, 1 % deionized formamide, 1x PCR buffer, and 2.5 U Taq DNA polymerase (Eurogentec, Belgium). Amplification reactions were run on a thermal cycler (VWR Unicyler, Gene Technologies Ltd, UK and Peltier Thermal Cycler, MJ Research INC, USA) using the cycling conditions as described previously

BGD
10, 15519–15557, 2013

(Díez et al., 2001). Amplicon fragment size and yield was determined by comparison with DNA smart ladder (Eurogentec, Belgium) on a 1 % agarose gel.

2.6 Denaturing gradient gel electrophoresis

DGGE analysis of the PCR products was carried out on a PhorU system (Ingeny, Goes, NL). Optimal fragment separation was obtained with a 15–55 % formamide-urea gradient (100 % denaturants defined as 7 M urea and 40 % formamide (Muyzer et al., 1993). For all samples we loaded 80 ng of PCR product with 1 % final concentration loading buffer (0.05 % w/v bromophenol blue, 40 % *w*/*v* sucrose, 0.1 M EDTA pH 8.0, 0.5 % sodium lauryl sulfate). For each sampling location, all samples were run on a single full DGGE (maximum of 40 samples on a 48-wells gel). An additional gel was run with samples from different locations, selected according to the temporal extremes of our data set, corresponding to early, mid and late spring. The polyacrylamide gels were silver stained (Heuer et al., 2001), dried (4 h, 60 °C), and scanned using a high resolution Epson Perfection V700 photo scanner (Epson, USA). DGGE fingerprints were analyzed using the Bio-Numerics® version 3.5 (Applied Maths). DGGE band patterns were digitalized and normalized using flanking marker samples. All positive bands (minimum 4 % profiling and 0.5 % surface area) were assigned to band classes, and the relative abundance was set to band surface (area under the Gaussian curve representing the band). The Pearson correlation coefficient (r) for each pair of lanes within a gel was calculated as a measure of similarity between the community profiles and the cluster analysis was performed by applying the unweighted pair group method with mathematical averages (UPGMA). Furthermore relative abundance data were used for diversity and multivariate analyses.

2.7 Sanger sequencing

We selected samples from our data set that represented early, mid, and late spring samples from Ocean (O), Kongsfjorden and Krossfjorden Glacier stations (G, KG). In

BGD
10, 15519–15557, 2013

total 10 surface samples were selected (09-04-08 Ocean; 14-04-08 Glacier; 16-04-08 Kross-Glacier; 06-05-08 Kross-Glacier; 12-05-08 Ocean & Kongs-Glacier; 21-06-07 Ocean & Kross-Glacier; 25-06-07 Kongs-Glacier) for generating clone libraries. All samples were amplified with the Euk1A-516R primer set as described above but using the GoTaq® HotStart Polymerase (Promega, Leiden, The Netherlands). PCR products (520bp fragments) were ligated to pGEM-t vector (Promega) and transformed into DH5α competent cells (Sylphium Life Sciences™, Groningen, The Netherlands). For each sample, 150–170 white colonies were selected and amplified from the vector's T7-SP6 sites. 30 ng of PCR product was cleaned using ExoSAP-IT (Affymetrix, Cleveland USA) and used as template in the sequencing reaction performed with BigDye® 3.1 Terminator buffers (Applied Biosystems) and 0.2 mM T7 primer. Sequences were run on an Applied Biosystems 3730xl Genetic Analyzer.

2.8 Sequence analysis

All sequences were manually checked and trimmed using Chromas software version 2.3 (Technelysium, Australia) and closest identity to other sequences was checked using NCBI BLAST. All suspected chimeric sequences were fragmented into smaller portions and run in BLAST. Chimeric sequences and fragments < 500 bp were excluded from the data set. Molecular Evolutionary Genetics Analysis (MEGA) version 4.0 (Tamura et al., 2007) and its add-in ClustalW was used to align the DNA sequences and to calculate pairwise DNA distance matrix using the Kimura-2-parameter model (Hartl et al., 1994; Zhu and Bustamante, 2005). All sequences were attributed to Operational Taxonomic Units (OTU) defined at the 97 % similarity level using MOTHUR software (Schloss et al., 2009). All sequences were submitted to the NCBI database (accession number KF534518 – KF534631).

BGD
10, 15519–15557, 2013

2.9 Meteorological data

Wind speed and direction, air temperature and irradiance were obtained from the AWIPEV observatory.

2.10 Data processing and statistical analysis

The attenuation coefficient for PAR (K_d) was calculated from linear regression on ln transformed irradiance data versus depth, and the 1 % depth for PAR was calculated. Diversity data were calculated using PAST software version 2.16 (Hammer et al., 2001). Statistical testing was run using Statistica 8.0. Student t tests and linear regressions (K_d, nutrient removal) were performed in Excel.

3 Results

3.1 Environmental conditions

Slight, yet significant sea surface salinity (SSS) differences were found in April–May (2008) within the Kongsfjorden. Station G surface waters showed a significantly lower surface salinity (t test, $p < 0.005$) with an average of 34.76 psu (±0.10), compared to O and M stations that had average surface salinities of 34.93 psu (±0.05) and 34.92 psu (±0.05), respectively. Station KG occasionally showed strongly reduced surface salinities, most likely caused by melting of observed sea-ice drifting within the inner Kongsfjorden. The late spring season of 2007 (May–June) showed significant meltwater effects: by mid-June surface water salinities had decreased considerably. The lowest surface salinity (SSS) 31.79 psu was recorded on 25 June near the Kongsfjorden Glacier. The freshwater inflow led to significantly lower SSS at all inner locations between 14 and 25 June at the G, M and KG stations (33.41 psu (±1.04), vs. 34.53 psu (±0.3), t test $p < 0.01$). Decreased surface salinities generally coincided with increased sea surface temperatures (Fig. 2) at all locations.

BGD
10, 15519–15557, 2013

On average, sea surface temperatures were significantly lower in 2008 (average $\mu = 0.63\,^{\circ}\mathrm{C} \pm 0.79$) than in 2007 ($\mu = 2.92\,^{\circ}\mathrm{C} \pm 1.07$); t test, $n = 68$, $t = 12{,}163$, $p < 0.001$) (Fig. 2). In spring 2008 (April–May) clear differences in water temperatures were observed between sampling stations. Ocean and Kongsfjorden Middle (stations O and M) stations had significantly higher temperatures than the Krossfjorden (stations KM and KG) and Kongsfjorden inner Glacier (station G) station ($\mu T_{\mathrm{O\cap M}} = 1.23\,^{\circ}\mathrm{C} \pm 0.35$; $\mu T_{\mathrm{Kr\cap G}} = -0.04\,^{\circ}\mathrm{C} \pm 0.58$; t test $p < 0.0001$).

3.2 Light attenuation

For all stations, vertical light attenuation (K_d) gradually increased over time, meaning that over time less light penetrated within the water column and lead to a shallower euphotic layer (Fig. 3). Both glacier stations (G, KG) showed enhanced K_d values already from the beginning of the season (April 2008 campaign), in particular near the Kongsfjorden glacier. The K_d coefficients for this station were significantly different from K_d's observed at the other stations (one-way ANOVA, $p < 0.01$). Here, K_d increased from $0.15\,\mathrm{m}^{-1}$ in early April to $1.22\,\mathrm{m}^{-1}$ at the end of spring in 2007. As a result 1 % light depths, which defines the euphotic layer boundary, decreased from 32 m in early April to 3.7 m at the end of the 2007 campaign (25 June) near the Kongsfjorden Glacier. Station KG also showed elevated K_d values as compared with the outer stations, ranging between $0.10\,\mathrm{m}^{-1}$ (early April) to $0.22\,\mathrm{m}^{-1}$ (21 June) (Fig. 3), leading to 1 % light depths decreasing from approximately 40 to 25 m during the course of the season. The middle fjord stations (M and KM) and station O had lowest K_d values at the start of the season in 2008 (K_d values of 0.063, 0.070, $0.077\,\mathrm{m}^{-1}$ for Ocean, M, and KM respectively), giving rise to 1 % light depths > 70 m. However, also at these stations K_d's increased right from the beginning of the season, up until 1 % light depths of 30 m, 12 m and 18 m, for Ocean, Middle (M) and Kross Middle (KM) respectively, at the end of the season.

BGD
10, 15519–15557, 2013

3.3 Nutrients

During the early spring campaign of 2008 nutrients generally showed a decreasing trend while during late spring (2007) nutrient concentrations remained stable but at low levels (Fig. 4). The 2007 nutrient concentrations were significantly lower than in 2008 for all nutrients (*t* test, $p < 0.001$). Maximum starting values at the beginning of the season were 11.3 µM for NO_x ($NO_3^{2-} + NO_2^-$), 0.83 µM for PO_4, and 4.8 µM for Si. Although a decreasing trend was observed at all stations, differences between stations were found. The strongest decrease in NO_x was observed at both Middle stations M and KM. The rate of nutrient decrease over time was calculated and given as removal rates (Table 1). In 2008, the highest NOx removal rates were 0.177 and 0.171 µmol L^{-1} d^{-1} for M and KM, respectively (0 and 20 m samples pooled). The other stations showed lower or no NO_x removal. At the Kongsfjorden glacier station no removal trend was found ($R^2 = 0.01$, Table 1), while samples from station KG showed a better fit ($R^2 = 0.92$) and much lower NOx removal rates as compared with the Middle and Ocean station. PO_4^{3-} removal was similar for all stations, ranging between 0.009 and 0.011 µmol L^{-1} d^{-1} (Table 1). In contrast, silicate removal varied greatly between stations, with the KG station showing the lowest (0.02 µmol L^{-1} d^{-1}), and station M the highest (0.072 µmol L^{-1} d^{-1}) removal rate (Table 1).

3.4 Phytoplankton biomass

Chlorophyll *a* concentration (µg L^{-1}) showed high variability in space and time. Chl *a* levels were relatively high in early spring (2008 campaign) at the Ocean and Middle Kongsfjorden Stations (Fig. 5 left panels, surface samples only). Nevertheless, in surface waters, chl *a* never exceeded 2.5 µg L^{-1}. A phytoplankton bloom seemed to develop during early spring at the Ocean and Middle Kongsfjorden stations, however, surface chl *a* concentrations dropped sharply in the third week of April (2008) (Fig. 5). On average, chl *a* concentrations were lower at stations G, KG and KM. For comparison, average chl *a* concentrations during the 2008 campaign were 1.25 (±0,74) µg L^{-1}

BGD
10, 15519–15557, 2013

for the Ocean station, and 0.35 (±0.26) µg L^{-1} and 0.19 (±0.09) µg L^{-1} for G and KG respectively. During the late spring campaign of 2007, chl *a* levels were low everywhere, ranging between 0.37 (±0.25) µg L^{-1} at station O, and 0.31 (±0.33) µg L^{-1} chl *a* at station G. No significant differences between 0 and 20 m chl *a* levels were found (results not shown).

3.5 Phytoplankton pigment fingerprints – CHEMTAX

The taxonomic composition of the phytoplankton as revealed by taxon specific pigment markers showed a high variability in space and time (Fig. 5, right panels). Similar to the chl *a* data, no significant differences were found between 0 and 20 m samples from the same location, therefore only surface patterns are shown (Fig. 5). In 4 samples from the Krossfjorden stations, 2008 campaign, pigment levels were too low ($\ll$ 0.1 µg Chl *a* L^{-1}) to detect the essential pigments required for a reliable CHEMTAX calculation. Pigment fingerprints showed that diatoms and haptophytes dominated in early spring (2008 campaign). These groups were replaced by other taxonomic groups during the late spring campaign (2007). Here (nano-) flagellates dominated as well as cyanobacteria, giving rise to a significantly enhanced fraction in the nano-pico size ranges (Fig. 5, left panels) (one-way ANOVA, $p < 0.0001$). Moreover, differences were found on the spatial scale. The highest relative abundance of diatoms and haptophytes was measured in the Ocean and Kongsfjorden Middle samples during early spring (2008) with the Ocean station showing the highest average diatom abundance during both campaigns (51 and 53 % in 2008, 2007 respectively). Remarkably, in 2008, the micro-phytoplankton composition at the glacier locations from both fjords and the Krossfjorden Middle station differed significantly from the Ocean and Kongsfjorden Middle stations, with lower relative amounts of diatoms and haptophytes (Tukey test, $p < 0.001$; $p < 0.005$), but enhanced fractions of chlorophytes, cryptophytes and cyanobacteria leading to an enhanced contribution of the nano-pico fractions (Fig. 5, left panels). Overall, at the end of the 2008 campaign (12 May) both outer stations (O, M) showed nano-pico fractions

BGD
10, 15519–15557, 2013

well below 10 %, while at the Kongs Glacier station in particular values above 30 % were found. At the start of the late spring campaign of 2007 this trend was also visible: the relative dominance of diatoms at the Ocean station decreased towards the inner parts of the fjords. At these inner locations, cryptophytes were highly abundant as well as cyanophytes. At the end of this campaign the nano-pico faction at the Ocean station had increased, which was mainly due to enhanced chlorophyte abundance, whereas cryptophyte abundance remained relatively low. Based on CHEMTAX, dinoflagellate abundance was never high, but a general increase in relative abundance was found during the late spring campaign, as compared with early spring. Qualitative microscopic analysis confirmed the CHEMTAX outcomes in particular with respect to cryptophyte presence at the glacier locations. Here small sized phytoplankton (cryptophytes, small dinoflagellates, occasional pennate diatoms) were often accompanied by small ciliates showing an average cell length of approximately 15 µm. At the end of the late spring campaign (19 and 21 June 2007, JD. 170 and 172) both glacier stations showed high numbers of cryptophytes in various sizes < 20 µm, whereas Ocean samples had numerous fragments of *Phaeocystis* colonies. During early spring (9 and 16 April 2008) the diatom community at this location consisted mainly of *Thalassiosira* spp., pennate chain forming diatoms, and *Chaetoceros* species in lower numbers. During late spring tintinnids and other ciliates of various sizes (< 20 µm, > 20 µm) were highly abundant at all locations.

3.6 Eukaryotic community – molecular fingerprints

DGGE was applied to all samples keeping samples from one location on separate gels. Similarity analysis of band patterns from a same sampling station generally showed clustering according to time and depth (data not shown). Ordination analysis and individual environmental variable testing confirmed that factors time, temperature, nutrients and depth significantly explained part of the variation observed for communities from a same sampling location.

BGD
10, 15519–15557, 2013

Pearson's similarity analysis of the band patterns of the additional gel containing samples from different locations and sampling days revealed two main clusters as shown in Fig. 6. The first cluster included samples with high band pattern diversity and a second cluster with lower band numbers. The high diversity cluster consisted of late spring (2007) samples collected at the onset of glacier melt water influence. Several 2008 samples were included within the "2007 cluster". Those 2008 samples were collected at stations G, KM and KG. Noticeably, within the "2007" cluster all fjord surface samples formed a distinct cluster from 20 m samples, indicative of stratification. This surface water cluster appeared to share strong similarity with 20 m samples collected on 25 June at the Kongsfjorden Glacier and Middle station. Overall, samples collected during early-mid spring from inner fjord stations appeared to share more similarity with glacier influenced late spring samples.

The cluster exhibiting lower diversity included exclusively 2008 samples. Furthermore there was a temporal and spatial separation between very spring and mid spring samples, representing a pre-bloom and a bloom community, respectively. The early spring (pre-bloom) samples included relatively more Krossfjorden samples, whereas the mid spring cluster consisted mostly of O and M station samples. The clustering suggests that the pre-bloom community was sustained longer in the Krossfjorden.

3.7 Molecular community composition – clone library sequencing

For each clone library we sequenced between 134 and 154 clones, yielding a total of 1457 sequences of a ±520 bp section of the 18S rRNA gene (position 1 to 520). From the 1457 sequences we identified 65 operational taxonomic units (OTU) at the 0.03 cut off level and 49 singletons. In Table 2 we list the environmental clone and the isolate sharing most identity with each OTU and the relative sequence distribution of each OTU for each sample. Overall we identified 760 *Alveolata* (*Dinophyeae*, *Syndiniales* and *Ciliophora*), 107 *Haptophyceae* (*Prymnesiales*), 66 *Viridiplantae* (*Chlorophyta*), 83 Stramenopiles (*Bacillariophyta*, *Pelagophyceae*, *Chrysophyceae*), 18 *Cryptophyta* (*Pyrenomonadales*), 12 *Picozoas* (formerly known as Picobiliphytes (Not et al.,

BGD
10, 15519–15557, 2013

2007; Seenivasan et al., 2013), 78 *Rhizaria* (*Cercozoa*, *Haplosporidia*), 15 *Telonema*, 15 *Choanoflagellida*, 249 *Metazoa* (*Maxillopoda*, *Annelida*, *Lophotrochozoa*, *Cnidaria*) related sequences. The sequence diversity was highest in Glacier samples from early April with a Shannon diversity index (H') of 2.82 and 3.19 for G and KG, respectively. Lowest diversity was found in Ocean samples from 12 May 2008 ($H' = 0.59$) and 30 April 2008 ($'H = 1.41$) that were dominated by copepod sequences.

The relative abundance of sequences identified as *Dinophyceae* was evenly distributed over the three locations and between different sampling days. Most *Haptophyceae* sequences were recovered in early spring samples from O and G samples, and then gradually decreased towards summer. *Haptophyceae* sequence distribution from clone libraries of the Krossfjorden Glacier samples was relatively evenly distributed over time. Sequences identified as Stramenopiles were mostly recovered from G and KG locations in early-mid spring. Chlorophyte sequences were mostly found in clone libraries from G ad KG locations in particular on the 12 May at location G.

Among sequences related to the grazer fraction of the community, copepod related sequences (*Calanus* sp. and *Oithona* sp.) were nearly exclusively recovered from Ocean samples from mid-spring 2008 (> 75 %). On the contrary, sequences related to *Ciliophora* were mostly recovered from G and KG locations, in particular from G samples from late spring. Clones identified as *Rhizaria* related sequences were mostly recovered from KG samples. Furthermore *Rhizaria* were overall more abundant in June samples, in particular in KG and O samples. Choanoflagellates were mostly recovered from mid-late spring samples, and absent in most early spring samples.

BGD
10, 15519–15557, 2013

4 Discussion

4.1 Comparison of phytoplankton community analysis methods: pigments, microscopy and 18SrRNA gene sequencing

In the present study we show that the combination of pigment and molecular fingerprinting, supported with occasional microscopic inspections, to assess phytoplankton community structure, are highly complementary. CHEMTAX analysis of taxon specific pigments revealed semi-quantitative differences in phytoplankton community structure at the class level over time and space. Incidental microscopy confirmed the quantitative data generated by the CHEMTAX analysis. For example, the high relative contribution of cryptophytes to total phytoplankton biomass, as revealed by CHEMTAX was confirmed by the high numbers of cryptophyte cells as visually observed for the glacier and late spring samples. Overall, the stations in close proximity to both glaciers, predominantly hosted a small cell community including cryptophytes, cyanobacteria, chlorophyll-b containing algae, and some pennate diatoms and small ciliates. The relatively high abundances of haptophyte and diatom specific pigments in early spring samples from the Ocean station were indeed observed by microscopy: samples were mainly composed of *Phaeocystis* sp. colonies and diatoms belonging to the genera *Thalassiosira*, *Fragilariopsis* and *Chaetoceros*. Furthermore, specific pigment signatures suggested a high relative contribution of cyanobacteria in some samples constituting up to 25 % of the total phytoplankton community. Confirmation of this finding was attempted by using specific cyanobacterial primers Cya27F1 and Cya809R (Jungblut et al., 2005, 2010; Lionard et al., 2012) on DNA extracts of the 0.2–2 µm size fraction. The amplification did not yield any specific cyanobacterial amplicons preventing the identification of cyanobacterial species present in the Kongs-Krossfjorden. Further investigation is therefore required to assess specific cyanobacterial presence and identity in both fjords.

Species composition inferred from partial 18S rRNA gene sequencing revealed a different community composition, as compared with CHEMTAX and microscopy. Most

BGD
10, 15519–15557, 2013

striking was a bias towards identification of Alveolate related sequences. Over half (760) of our 1454 environmental sequences were identified as *Alveolata*, among which 591 were most related to the *Dinophyceae*. Alveolates are known to often dominate in 18S rRNA gene libraries (Massana and Pedrós-Alió, 2008). Clone libraries of the 18S rRNA gene are mostly biased towards high 18S rRNA gene copy number species (Zhu et al., 2005). Other Arctic studies on marine protistan communities also observed a large dominance of Alveolata related sequences (Lovejoy et al. 2006, Terrado et al., 2011). Analysis of protistan rRNA gene clone libraries from the Amundsen Gulf (Canadian Arctic) showed that rRNA gene clone libraries mostly consisted of OTUs identified as *Ciliophora*, *Dinophyceae*, Marine *Alveolata*, which are all members of the Alveolate superphyla, and furthermore Marine Stramenopile (MAST) and Prasinophyte OTUs.

In addition to the high contribution of Alveolate related sequences, a striking difference with the CHEMTAX approach was the underrepresentation of diatom (Stramenopile) and the near absence of cryptophyte sequences. This underlines that when solely applying molecular methods, the phytoplankton community is not realistically reflected by analysis of the 18S rRNA gene. On the other hand analysis of the 18S rRNA gene also has an important added value since it provides information on non-pigmented species and on the identity of taxonomically unidentifiable smaller species belonging to relevant marine taxonomic groups such as chlorophytes, prasinophytes, picozoa, haptophytes, chrysophytes and pelagophytes, as demonstrated for the two Arctic fjords under study (Table 2). Moreover, 18S rRNA gene sequencing provided qualitative information on smaller heterotrophs belonging to the Ciliophora, Syndiniales, Choanoflagellates, Cercozoa, and Telonema. High throughput sequence analysis of RNA instead of the 18S rRNA gene might provide a more accurate reflection of the active/live part of the plankton community. In addition, it has been proposed that RNA based libraries are more representative of environmental conditions prevailing at the time of sampling (Stoeck et al., 2007). For future protistan and phytoplankton community studies we recommend the sequencing of rRNA and RNA libraries through

BGD
10, 15519–15557, 2013

next generation sequencing methodologies and complementary taxon specific pigment analysis.

4.2 Kongsfjorden springtime phytoplankton dynamics

Typically, Kongsfjorden spring blooms peak in May and consist of *Phaeocystis pouchetii* and diatoms (*Thalassiosira* spp., *Chaetoceros* spp. and *Fragilariopsis* spp.) (Hegseth and Tverberg, 2013; Hodal et al., 2012; Seuthe et al., 2011). However, in recent years, the bloom timing varied from April to the end of May (Hegseth and Tverberg, 2013). Shifts in bloom timing have been attributed to the variable presences of sea ice and anomalous wintertime Atlantic Water (AW) inflow events into the fjord. The mooring site within the Kongsfjorden revealed important wintertime AW inflow events in three consecutive years (2006–2008) (Hegseth and Tverberg, 2013). In our sampling years of 2007 and 2008 the winter cooling of the fjord was interrupted by several AW incursions in surface waters. Hegseth and Tverberg (2013) reported decreased spring bloom chl *a* values and altered taxonomic composition during the bloom period. The composition shift was most pronounced during the 2007 spring bloom with a *Phaeocystis pouchetii* dominated community (> 90 %) complemented by small flagellates and only a minor contribution of diatoms (1 %). The bloom was delayed to mid-May and strongly reduced in duration. By the 23 May only 10 % of the bloom remained, and the succession towards a flagellate community had started. These data enabled us to situate our 2007 late spring sampling period (22 May to 25 June) within the post-bloom period. Kongsfjorden phytoplankton succession has been reported to shift to a nano- and picoplankton and dinoflagellate dominated community during summer (Keck et al., 1999; Rokkan Iversen and Seuthe, 2011; Seuthe et al., 2011). Our 2007 data showed that haptophyte and diatom pigments, which normally constitute the largest fraction of the spring community (Fig. 5), had mostly disappeared although fragments of senescent *Phaeocystis* colonies were still observed at the O and M stations. Moreover, the late spring 2007 nutrient data showed largely nutrient depleted surface waters. Despite the relatively diatom-poor 2007 bloom reported by Hegseth and Tverberg (2013), our

BGD
10, 15519–15557, 2013

late spring nutrient data also showed silica concentrations below 2 µM, suggesting that diatoms might have peaked earlier than the *Phaeocystis* sp. bloom, in- or outside the Kongsfjorden. The observed succession from haptophytes and diatoms to the nano- and picophytoplankton sized classes (chlorophytes, cryptophytes, dinoflagellates and cyanobacteria) is in agreement with other studies conducted in the Kongsfjorden during late spring and summer (Keck et al., 1999; Rokkan Iversen and Seuthe, 2011; Seuthe et al., 2011).

In 2008, Hegseth and Tverberg (2013) measured an increase in chl *a* (up to 1.6–1.9 µg L^{-1}) between 18 and 21 April (JD's 109 to 112) at the central Kongsfjorden monitoring site. They speculated that this was the initiation of the spring bloom, composed of *Phaeocystis* sp. (90 %) and diatoms (7 %), (*Fragilariopsis* sp., *Thalassiosira* spp., *Chaetoceros* sp. and pennate diatoms). Our early April CHEMTAX and microscopy data showed similar taxonomic composition and maximal chl *a* values at the Ocean station of 1.7 µg L^{-1} on 16 April (JD 107). From mid April 2008 onwards the spring bloom did not develop steadily at all fjord locations. Chl *a* values in Kongsfjorden Middle station showed a small increase around the 19 April to 0.7 and 1 µg L^{-1} in surface waters and 20 m samples, respectively, whereas chl *a* levels from all other stations stayed below 0.5 µg L^{-1}. Between the 19 and 26 April we measured a sharp decrease in chl *a* at the Ocean and Middle station, dropping down to < 0.5 µg L^{-1}. This coincided with a high wind velocity period of 4 days (daily average wind speeds 6.95 and 8.2 m s^{-1}) from NWW direction, which freely blew into the Kongsfjorden which has a North West-South East orientation. The high winds combined with low air temperatures (wind chill −37 °C) likely caused vertical mixing and cooling of the water column. This was confirmed by the CTD profiles (Fig. 2) showing a homogeneous water column for the upper 60 m at the O and M stations. The resultant vertical redistribution of phytoplankton biomass may have interrupted bloom formation, and could cause changes in phytoplankton composition, as found before (Hegseth and Tverberg, 2013; Piquet et al., 2011). After the wind event, a period characterized by relatively calm southerly winds permitted stabilization of the water column and therefore biomass build up. Chl *a*

BGD
10, 15519–15557, 2013

values eventually increased after the 28 April up to our last sampling day on the 12 May, reaching up to 2.5 and 2.8 µg L^{-1} at the Ocean station at 0 and 20 m, respectively, and 2 and 2.5 µg L^{-1}, at 0 and 20m depth respectively, on 2 May, at Kongsfjorden Middle station. Maximal chl *a* values from our data were still well below maximal chl*a* spring time values that can reach up to ∼ 13 µg L^{-1} as recorded in other years (Hegseth and Tverberg, 2013; Hop et al., 2002). This indicates that the 2008 spring bloom was disrupted and characterized by low biomass throughout.

4.3 Cyanobacteria as potential marker species

Our pigment data are the first showing the relative importance of cyanobacteria in Kongsfjorden-Krossfjorden. Cyanobacteria are ubiquitous and important contributors to primary production in warmer waters, and were long considered to be absent from high latitude polar waters (Partensky et al., 1999). Yet, more recently a few studies have observed cyanobacteria in Arctic waters. Cottrell and Kirchman (2009) found *Synechococcus* spp. in samples from the Chukchi and Beaufort Sea. While, Diez et al. (2012) reported the presence of cyanobacterial *NifH* genes in samples collected in the Fram Strait, west from Spitsbergen. We propose that the regular Atlantic water incursions might have contributed to transport of cyanobacterial species from the milder Atlantic currents into the Kongsfjorden. A temperate origin for the Chukchi and Beaufort Sea *Synechococcus* spp. was also proposed by Cottrell and Kirchman (2009). In the past, Atlantic water inflow events have been associated with observations of the haptophyte *Emiliania huxleyi* in Svalbard and Arctic waters (Hasle and Heimdal, 1998; Hegseth and Sundfjord, 2008; Hop et al., 2002). As a result, this species was proposed as a marker species for AW intrusion in the area. However in our 2007 and 2008 samples, two years with strong AW influence, no *E. huxleyi* cells were found. Instead, cyanobacterial presence might be a more promising AW marker as suggested earlier (Gradinger and Lenz, 1989).

BGD
10, 15519–15557, 2013

4.4 Influence of environmental conditions on springtime phytoplankton biomass and composition

Differences in both phytoplankton biomass (chl *a*) and composition between stations Ocean and Kongsfjorden Middle versus Krossfjorden Middle and both Glacier stations were striking. The inner locations had significantly lower chl *a* values, and showed a higher relative abundance of nano-picoplankton groups throughout the early spring sampling period. At the Ocean site, 2008 chl *a* values and diatom pigments were positively correlated (ln transformed chl *a*; $y = 32.407x + 56.815$, $R^2 = 0.736$). Other locations showed relatively low diatom pigment concentrations. Diatoms are considered primary biomass contributors in polar waters (Varela et al., 2002) and their relative lower contribution at Kongsfjorden Glacier and Krossfjorden stations probably was an important determinant for lower chl *a* values. In support of this, Rokkan Iversen and Seuthe (2011), showed a low contribution of < 10 µm sized cells (expressed as % chl *a*) during the spring bloom at their monitoring location in the central Kongsfjorden, while comprising the largest fraction of the phytoplankton (75–95 %) during the rest of the year.

The Kongsfjorden and Krossfjorden Glacier locations showed lower water temperatures with sub zero values. We speculate that the prevailing lower water temperatures prevented the development of a spring bloom at those locations. On the other hand, the nutrient data demonstrated uptake and hence phytoplankton growth at these locations although the observed lower silica uptake rates indicated decreased quantitative importance of diatoms. The Kongsfjorden Glacier data showed a highest chl *a* value of 0.8 µg L^{-1} on the 5 May, corresponding with an intrusion event of saltier and warmer water (Fig. 2, JD 124) and thus probably reflecting transport of phytoplankton from the Middle Station.

In addition to the relatively colder conditions, inner fjord locations were also characterized by lower salinities. The surface waters at the Krossfjorden glacier station were significantly fresher due to sea ice melting leading to surface stratification (Fig. 2) dur-

BGD
10, 15519–15557, 2013

ing early spring (2008 campaign). Salinities near the Kongsfjorden Glacier also showed slightly reduced values during the 2008 campaign. Sea ice was largely absent from the Kongsfjorden, and reduced salinities were probably caused by early spring time glacier melting. The overall significantly higher K_d values measured near the glacier support an early onset of glacier meltwater, enriched in sediment particles, during early spring. Several other polar studies have reported shifts in phytoplankton communities towards smaller sized phytoplankton species, as a result of meltwater input. Along the Western Antarctic Peninsula reduced water salinities were correlated to increased cryptophytes abundance (Moline et al., 2004), whereas diatom and prymnesiophytes were associated to saltier water masses. The relatively higher proportion of nano-picoplankton at the inner fjord locations during spring time could have been partially mediated by glacier influence expressed in lower salinities and temperatures. Also, it cannot be ruled out that meltwater induced surface stabilization that caused rapid sinking of diatoms out of the euphotic zone, the latter becoming highly shallow towards the end of spring. In addition, the sub optimal irradiance conditions resulting from strong light attenuation near the Glaciers, could also have limited phytoplankton growth. Our molecular fingerprinting data further support the hypothesis that early glacier influence was at hand, as spring phytoplankton community fingerprints from inner fjord stations shared more similarity to late spring communities, than the outer fjord spring community. The transect data from Hegseth and Tverberg (2013) from spring 2006 show an early spring bloom with high chl *a* concentrations ($13\,\mu g\,L^{-1}$) measured in the Kongsfjorden in particular at stations Kb0–Kb2 corresponding to our Ocean and Middle station, whereas the inner Kongsfjorden (Kb5) corresponding to our Glacier station had much lower chl *a* concentrations ($< 5\,\mu g\,L^{-1}$). In other words, even during a high phytoplankton biomass season, glacier proximity appears to limit biomass.

BGD
10, 15519–15557, 2013

5 Conclusion

In the present study we generated a data set enabling a comparison in phytoplankton springtime dynamics and composition between the two adjacent fjords. Our results show that despite their shared Ocean connection and their apparent proximity, springtime phytoplankton dynamics differ significantly between the fjords, as was proposed before for summertime communities (Piquet et al., 2010). Our springtime mini-transect survey show that Kongs- and Krossfjorden springtime phytoplankton conditions are strongly governed by Oceanic as well as glacier influence. Both are fed by numerous glaciers, but the sediment discharge is more important in the inner Kongsfjorden. Furthermore, the Kongsfjorden appeared to be more influenced by AW inflow, mediating higher water temperatures, whereas the Krossfjorden stayed much colder throughout early spring, and shared much resemblance to the inner Kongsfjorden conditions. These physical differences appeared to affect the development of phytoplankton biomass. Near glacier vicinity conditions influenced phytoplankton community composition as early as spring, with a limited biomass buildup, a relatively smaller sized phytoplankton community, resembling late spring communities sampled within glacier meltwater plumes. Our microscopy and sequence analysis suggest that the grazer community composition is also affected. Copepods were dominating in outer station locations, where diatoms and *Phaeocystis* sp. dominated, whereas ciliates were the dominant grazer fraction at inner fjord locations. From this we can speculate that an earlier onset of glacier melting in spring will limit biomass buildup, facilitate a smaller sized phytoplankton community, mostly grazed by ciliates which may channel organic carbon towards the microbial loop, rather than to higher trophic levels. We therefore conclude that ongoing climate change, leading to more Atlantic Water intrusions in the Kongsfjorden and an early glacier meltwater onset will affect phytoplankton biomass, composition and thus may have a cascading effect on the fate of organic carbon hence on biogeochemical carbon cycling.

BGD
10, 15519–15557, 2013

Acknowledgements. This research was financed by NWO, as part of the IPY-PAME framework. Field work at Koldeway station was supported and financed by AWI. We thank the Kings Bay AS. personnel, in particular the captain of MS Teisten and the Kings Bay Marine Laboratory manager, for their excellent logistic support. Nutrient analyses were run at the NIOZ by Jan van Ooijen. We are grateful for the microscopy analyses performed by Loes A. H. Venekamp.

References

Buchholz, F., Buchholz, C., and Weslawski, J. M.: Ten years after: krill as indicator of changes in the macro-zooplankton communities of two Arctic fjords, Polar Biol., 33, 101–113, 2010.

Cottier, F., Tverberg, V., Inall, M., Svendsen, H., Nilsen, F., and Griffiths, C.: Water mass modification in an Arctic fjord through cross-shelf exchange: the seasonal hydrography of Kongsfjorden, Svalbard, J. Geophys. Res. C, 110, 1–18, 2005.

Cottrell, M. T. and Kirchman, D. L.: Photoheterotrophic Microbes in the Arctic Ocean in Summer and Winter, Appl. Environ. Microb., 75, 4958–4966, 2009.

Coupel, P., Jin, H. Y., Joo, M., Horner, R., Bouvet, H. A., Sicre, M.-A., Gascard, J.-C., Chen, J. F., Garçon, V., and Ruiz-Pino, D.: Phytoplankton distribution in unusually low sea ice cover over the Pacific Arctic, Biogeosciences, 9, 4835–4850, doi:10.5194/bg-9-4835-2012, 2012.

Díez, B., Pedrós-Alió, C., Marsh, T., and Massana, R.: Application of denaturing gradient gel electrophoresis (DGGE) to study the diversity of marine picoeukaryotic assemblages and comparison of DGGE with other molecular techniques, Appl. Environ. Microb., 67, 2942–2951, 2001.

Díez, B., Bergman, B., Pedros-Alio, C., Anto, M., and Snoeijs, P.: High cyanobacterial nifH gene diversity in Arctic seawater and sea ice brine, Environ. Microbiol. Rep., 4, 360–366, 2012.

Gradinger, R. and Lenz, J.: Picocyanobacteria in the High Arctic, Mar. Ecol.-Prog. Ser., 52, 99–101, 1989.

Hammer, O., Harper, D. A. T., and Ryan, P. D.: PAST: Paleontological statistics software package for education and data analysis, Palaeontol. Electron., 4, 38–47, 2001.

Hartl, D. L., Moriyama, E. N., and Sawyer, S. A.: Selection intensity for codon bias, Genetics, 138, 227–234, 1994.

BGD
10, 15519–15557, 2013

Hasle, G. R. and Heimdal, B. R.: The net phytoplankton in Kongsfjorden, Svalbard, July 1988, with general remarks on species composition of arctic phytoplankton, Polar Res., 17, 31–52, 1998.
Hegseth, E. N. and Sundfjord, A.: Intrusion and blooming of Atlantic phytoplankton species in the high Arctic, J. Marine Syst., 74, 108–119, 2008.
Hegseth, E. N. and Tverberg, V.: Effect of Atlantic water inflow on timing of the phytoplankton spring bloom in a high Arctic fjord (Kongsfjorden, Svalbard), J. Marine Syst., 113–114, 94–105, 2013.
Heuer, H., Wieland, J., Schönfeld, J., Schönwäalder, A., Gomes, N. C. M. and Smalla, K.: Bacterial community profiling using DGGE and TGGE analysis, in: Environmental molecular microbiology: protocols and applications, edited by: Rouchelle, P., Horizon Scientific Press, Hymondham, UK, 177–190, 2001.
Hodal, H., Falk-Peterson, S., Hop, H., Kristiansen, S., and Reigstad, M.: Spring bloom dynamics in Kongsfjorde, Svalbard: nutrients, phytoplankton, protozoans and primary production, Polar Biol., 35, 191–203, 2012.
Hop, H., Pearson, T., Hegseth, E. N., Kovacs, K. M., Wiencke, C., and Kwasniewski, S.: The marine ecosystem of Kongsfjorden, in Svalbard, Polar Res., 21, 167–208, 2002.
Hop, H., Falk-Peterson, S., Svendsen, H., Kwasniewski, S., Pavlov, V., Pavlova, O., and Soride, J. E.: Physical and biological characteristics of the pelagic system across Fram Strait to Kongsfjorden, Prog. Oceanogr., 71, 182–231, 2006.
Jungblut, A., Hawes, I., Mountfort, D., Hitzfeld, B., Dietrich, D., Burns, B., and Neilan, B.: Diversity within cyanobacterial mat communities in variable salinity meltwater ponds of McMurdo Ice Shelf, Antarctica, Environ. Microbiol., 7, 519–529, 2005.
Jungblut, A. D., Lovejoy, C., and Vincent, W. F.: Global distribution of cyanobacterial ecotypes in the cold biosphere, ISME J., 4, 191–202, 2010.
Keck, A., Wiktor, J., Hapter, R., and Nilsen, R.: Phytoplankton assemblages related to physical gradients in an arctic, glacier-fed fjord in summer, ICES J. Mar. Sci., 56, 203–214, 1999.
Li, W. K. W., McLaughlin, F. A., Lovejoy, C., and Carmack, E. C.: Smallest algae thrive as the Arctic Ocean freshens, Science, 326, 539–539, 2009.
Lionard, M., Pequin, B., Lovejoy, C., and Vincent, W. F.: Benthic cyanobacterial mats in the high arctic: multi-layer structure and fluorescence responses to osmotic stress., Front. Microbiol., 3, 140, 2012.

BGD
10, 15519–15557, 2013

Lovejoy, C., Massana, R., and Pedrós-Alió C.: Diversity and distribution of marine microbial eukaryotes in the Arctic Ocean and adjacent seas, Appl. Environ. Microb., 72, 3085–3095, 2006.

Mackey, M. D., Mackey, D. J., Higgins, H. W., and Wright, S. W.: CHEMTAX – a program for estimating class abundances from chemical markers: application to HPLC measurements of phytoplankton, Mar. Ecol.-Prog. Ser., 144, 265–283, 1996.

Massana, R. and Pedrós-Alió, C.: Unveiling new microbial eukaryotes in the surface ocean, Curr. Opin. Microbiol., 11, 213–218, 2008.

Moline, M., Claustre, H., Frazer, T., Schofield, O. and Vernet, M.: Alteration of the food web along the Antarctic Peninsula in response to a regional warming trend, Glob. Change Biol., 10, 1973-1980, 2004.

Montes-Hugo, M., Doney, S. C., Ducklow, H. W., Fraser, W., Martinson, D. G., Stammerjohn, S. E., and Schofield, O.: Recent changes in phytoplankton communities associated with rapid regional climate change along the Western Antarctic Peninsula, Science, 323, 1470, 2009.

Muyzer, G., de Waal, E. C., and Uitterlinden, A. G.: Profiling of complex microbial populations by denaturing gradient gel electrophoresis analysis of polymerase chain reaction-amplified genes coding for 16S rDNA, Appl. Environ. Microb., 59, 695–700, 1993.

Not, F., Valentin, K., Romari, K., Lovejoy, C., Massana, R., Töbe, K., Vaulot, D., and Medlin, L. K.: Picobiliphytes: a marine picoplanktonic algal group with unknown affinities to other eukaryotes, Science, 315, 352–355, 2007.

Partensky, F., Blanchot, J., and Vaulot, D.: Differential distribution and ecology of *Prochlorococcus* and *Synechococcus* in oceanic waters: a review, in: Marine Cyanobacteria, edited by: Charpy, L. and Larkum, A. W. D., Institute of Oceanography, Monaco, 457–475, 1999.

Piquet, A. M. T., Scheepens, J. F., Bolhuis, H., Wiencke, C., and Buma, A. G. J.: Variability of protistan and bacterial communities in two Arctic fjords (Spitsbergen), Polar Biol., 33, 1521–1536, 2010.

Piquet, A. M. T., Bolhuis, H., Meredith, M. P., and Buma, A. G. J.: Shifts in coastal Antarctic marine microbial communities during and after melt water-related surface stratification, FEMS Microbiol. Ecol., 76, 413–427, 2011.

Rokkan Iversen, K. and Seuthe, L.: Seasonal microbial processes in a high-latitude fjord (Kongsfjorden, Svalbard): I. Heterotrophic bacteria, picoplankton and nanoflagellates, Polar Biol., 34, 731–749, 2011.

BGD
10, 15519–15557, 2013

Schlichtholz, P. and Goszczko, I.: Interannual variability of the Atlantic water layer in the West Spitsbergen Current at 76.5° N in summer 1991–2003, Deep-Sea Res. Pt. I, 53, 608–626, 2006.

Schloss, P. D., Westcott, S. L., Ryabin, T., Hall, J. R., Hartmann, M., Hollister, E. B., Lesniewski, R. A., Oakley, B. B., Parks, D. H., Robinson, C. J., Sahl, J. W., Stres, B., Thallinger, G. G., Van Horn, D. J., and Weber, C. F.: Introducing mothur: Open-Source, Platform-Independent, Community-Supported Software for Describing and Comparing Microbial Communities, Appl. Environ. Microb., 75, 7537–7541, 2009.

Seenivasan, R., Sausen, N., Medlin, L. K., and Melkonian, M.: Picomonas judraskeda gen. et sp. nov.: the first identified member of the Picozoa phylum nov., a widespread group of picoeukaryotes, formerly known as "picobiliphytes", PloS one, 8, e59565, doi:10.1371/journal.pone.0059565, 2013.

Seuthe, L., Rokkan Iversen, K., and Narcy, F.: Microbial processes in a high latitude fjord (Kongsfjorden, Svalbard): II Ciliates and dinoflagellates, Polar Biol., 34, 751–766, 2011.

Stoeck, T., Zuendorf, A., Breiner, H., and Behnke, A.: A molecular approach to identify active microbes in environmental eukaryote clone libraries, Microbiol. Ecol., 53, 328–339, 2007.

Svendsen, H., Beszczynska-Møller, A., Hagen, J. O., Lefauconnier, B., Tverberg, V., Gerland, S., Ørebæk, J. B., Bischof, K., Papucci, C., Zajaczkowski, M., Azzolini, R., Bruland, O., Wiencke, C., Winther, J., and Dallman, W.: The physical environment of the Kongsfjorden-Krossfjorden, an arctic fjord system in Svalbard, Polar Res., 21, 133–166, 2002.

Tamura, K., Dudley, J., Nei, M., and Kumar, S.: MEGA4: Molecular Evolutionary Genetics Analysis (MEGA) software version 4.0, Mol. Biol. Evol., 24, 1596–1599, 2007.

Terrado, R., Medrinal, E., Dasilva, C., Thaler, M., Vincent, W. F., and Lovejoy, C.: Protist community composition during spring in an Arctic flaw lead polynya, Polar Biol., 34, 1901, 2011.

Varela, M., Fernandez, E. and Serret, P.: Size-fractionated phytoplankton biomass and primary production in the Gerlache and south Bransfield Straits (Antarctic Peninsula) in Austral summer 1995–1996, Deep-Sea Res. Pt. II., 49, 749–768, 2002.

Zhu, F., Massana, R., Not, F., Marie, D., and Vaulot, D.: Mapping of picoeukaryotes in marine ecosystems with quantitative PCR of the 18S rRNA gene, FEMS Microbiol. Ecol., 52, 79–92, 2005.

Zhu, L. and Bustamante, C. D.: A composite-likelihood method for detecting directional selection from DNA sequence data, Genetics, 170, 1411–1421, 2005.

BGD
10, 15519–15557, 2013

Table 1. Early spring nutrient removal rates.

Station	NO_x	PO_4^{3-}	SiO_3^{2-}
Ocean (O) (n = 18)	−0.158 (0.44)	−0.011 (0.57)	−0.057 (0.27)
Kongs Middle (M) (n = 20)	−0.177 (0.58)	−0.011 (0.80)	−0.072 (0.46)
Kongs Glacier (G) (n = 16)	−0.057 (0.01)	−0.010 (0.33)	−0.060 (0.37)
Kross Middle (KM) (n = 8)	−0.171 (0.91)	−0.009 (0.89)	−0.052 (0.50)
Kross Glacier (KG) (n = 8)	−0.147 (0.92)	−0.009 (0.87)	−0.027 (0.51)

NO_x, PO_4^{3-} and SiO_3^{2-} removal (μmol L^{-1} d^{-1}) over time for the 5 stations, based on linear regression analysis of dissolved nutrients for 0 and 20 m samples (pooled) of 2008 samples. (R^2 : regression coefficient).

BGD
10, 15519–15557, 2013

Table 2. Distribution, classification, blast results related to the 64 operational taxonomic units identified at the 0.03 cut off level.

OTU (Sva_)	O 0904	O 3004	O 1205	O 2106	G1404	G 1205	G 2506	kG 1604	kG 0605	kG 2106	ALL	CLASSIF	ISOLATE	ENVIRONMENTAL CLONE
G1404-1097	19	6		2	21	4		9	17	6	**84**	HAP; Phaeo	Phaeocystis pouchetii isolate P360 AF182114	~
G1205-0183				1	2	5	1	2		4	**15**	HAP; Prym	Chrysochromulina simplex AM491021	*umec* pico HM581636
G2506-1002						2	4			2	**8**	HAP; Prym	Chrysochromulina leadbeateri AM491017	u mar euk B28-0201 JF273973
	19	***6***	***0***	***3***	***23***	***11***	***5***	***11***	***17***	***12***	***107***	TOTAL HAPTOPHYCEAE		
kG1604-1259	1				5	2		6		1	**15**	STR; Bacil; Med	Odontella sinensis strain CCMP1815 HQ912564	u picopl cl. BK401 GU433181 NSea
kG1604-1318	2				3			10			**15**	STR; Bacil; Cos	Thalassiosira antarctica CCMP982 DQ514874	~
G2506-1026							8			1	**9**	STR; Bacil; Cos	Chaetoceros sp. ArM0005 EU090014	~
G1404-1142	1				2	1				2	**6**	STR; Bacil; Frag	Synedra minuscula CCMP845 EF423415	*umec* BK298 GU433125 Nsea
kG1604-1264	1							6			**6**	STR; Bacil; Cos	Corethron inerme AJ535180	~
kO0904-0055	2				1	1		1			**5**	STR; Bacil; Baci	Pleurosigma intermedium AY485489	~
G2506-0973					1		2				**3**	STR; Bacil; Cos	Skeletonema grevilleii CCMP 1685 DQ396512	~
kG1604-1287								2			**2**	STR; Bacil; Med	Brockmanniella brockmannii CCMP151 HQ912565	u stramenopile cl 70S8Be8Op JQ782032
G1205-0193						4				1	**5**	STR; Chry	Spumella sp. Mbc_3C AB425951	u freshwater cl LG20-09 AY919752
G1205-0271						3					**3**	STR; Laby	Aplanochytrium sp. S1a FJ810216	u picoeuk cl. ws_138, 1804D11 FR874462
G1205-0265	1				4	5			1	1	**12**	STR; Pelag	Pelagococcus subviridis PSU14386	umec SGYH1519.FRAG.MO.500m JX842329 ENPaci
G1404-1056					1					1	**2**	STR; Pelag	Aureococcus anophagefferens JQ420083	~
	8	***0***	***0***	***0***	***17***	***16***	***10***	***25***	***1***	***7***	***83***	TOTAL STRAMENOPILES		
G1205-0220		1		1	3	21	5	2	3	3	**39**	VIR; Chlor; Mam	Mantionella squamata X73999	~
kG1604-1308	2			3	3	3		5	2		**18**	VIR; Chlor; Prasi	Pyramimonas gelidicola HQ111511	*umec* Q3-30 JQ420120
G1205-0244						5	1	1		2	**9**	VIR; Chlor; Mam	Bathycoccus prasinos FN562453	umec SGUH466.FRAG.MO.5m JX841666 ENPaci
	2	***1***	***0***	***4***	***6***	***29***	***6***	***8***	***5***	***5***	***66***	TOTAL VIRIDIPLANTAE		
kG2106-0862	1					1	2			8	**12**	PICOBI	Picobiliphyte sp. MS584-11 JN934891	umec SGYH1057.FRAG.MO.500 m JX842028 ENPaci
O0904-0135	11							2			**13**	CRYP; Pyren	Geminigera cryophila JF791030	umc picopl ws_159, 1815F07 FR874747 Fjord
kG2106-0839							1			2	**3**	CRYP; Pyren	Geminigera cryophila DQ452092	u cryptophye cl. env_Pavin_epi_T_NS21Gbis (freshwater) JX869382
O0904-0009	2										**2**	CRYP; Pyren	Geminigera cryophila JF791030	uec NPK97_252 EU371367 Kongsfjorden
	13	***0***	***0***	***0***	***0***	***0***	***1***	***2***	***0***	***2***	***18***	TOTAL CRYPTOPHYTA		
kG0605-0461	5		1	47	29	50	26	5	82	19	**264**	ALV; Dino; Gymn	Gyrodinium cf. Gutrula FN669511	umec CNCIII05_47 HM581708 Centr Arc Oce
O3004-1454	39	57	10	12	16	5	7	24	26	8	**204**	ALV; Dino; Gymn	Gyrodinium spirale AB120001	umec SGUH845.FRAG.MO.5m JX841912 ENPaci
kG2106-0859	6	1		7	1		2			20	**37**	ALV; Dino; Sues	Gymnodinium beii GBU41087	*uec* :49 AB510387 Suribati lake Arctic Sediment
O0904-0078	14				2						**16**	ALV; Dino; Gymn	Karlodinium micrum JF791049	umec. SGYH416.FRAG.MO.500m JX842362 ENPaci
O2106-0669	1			6	2			2	2	3	**16**	ALV; Dino; Gymn	Lepidodinium viride JF791033	u picopl cl. BK071 GU433177 NSea
kG1604-1253							3	5		2	**10**	ALV; Dino; Gymn	Lepidodinium viride AF022199	*umec* CNCIII51_17 HM581762 Centr Arctic Ocean
kG1604-1271	1			1	1	1		3	2	1	**10**	ALV; Dino; Gymn	Karlodinium micrum JF791049	*umec* ws_164, clone 1816E11 FR874810 Fjord
kG2106-0847				1			1	1	1	4	**8**	ALV; Dino; un.	Dinophyceae sp. CCMP1878 AY251287	umec SGUH638.FRAG.MO.5m JX841784 ENPaci
O0904-0123	3	1									**4**	ALV; Dino; un.	Dinophyceae sp. Jeong2006-1 AM408889	u Syndiniales cl. BIO1_F7 FN598232
kG1604-1238	1							3			**4**	ALV; Dino; Peri	Pentapharsodinium tyrrhenicum AF022201	umec. SGYH1536.FRAG.MO.500m JX842339 ENPaci
kG1604-1281	1							2			**3**	ALV; Dino; Peri	Roscoffia capitata AF521101	umec SGYH772.FRAG.MO.500m JX842549 ENPaci
kG1604-1298					1			2			**3**	ALV; Dino; Gony	Azadinium spinosum JX262491	umec SGUH1151.FRAG.MO.5m JX841415 ENPaci
G2506-0902							2				**2**	ALV; Dino; Peri	Heterocapsa triquetra AJ415514	umec PROSOPE99.CTD2.30m.141203_16 DQ001453
kG1604-1315							1	1			**2**	ALV; Dino; un.	Dinophyceae sp. RS-24 AY434686	umec SGYH921.FRAG.MO.500m JX842636 ENPaci
O0904-0033	2										**2**	ALV; Dino; Peri	Lessardia elongata AF521100	umec SGYH772.FRAG.MO.500m JX842549 ENPaci
G2506-0997							1		1		**2**	ALV; Dino; Gymn	Gyrodinium rubrum AB120003	umec SGUH510.FRAG.MO.5m JX841692 ENPaci
O1205-0335			2								**2**	ALV; Dino; Peri	Protoperidinium americanum AB716911	umec E4-160 ANT Davis EU078319 EAnt Davis
kG2106-0889										2	**2**	ALV; Dino; Peri	Protoperidinium bipes AB284159	~
G1205-0236						5			2		**7**	ALV; Dino; Syn	Amoebophrya sp. AY208893	u alv c RA001219.16 DQ186528
G1404-1107	1				5						**6**	ALV; Dino; Syn	Amoebophrya sp. AF47255	umec SGUH1446.FRAG.MO.5m JX841564 ENPaci
G2506-0975	1					1	2				**4**	ALV; Dino; Syn	Amoebophrya sp. AY208893	uec B19bE11 EU333058
kG1604-1313					1			3			**4**	ALV; Dino; Syn	Amoebophrya sp. AY775285	u picopl ec BK161 GU433113
kG1604-1240								1	1		**2**	ALV; Dino; Syn	Amoebophrya sp. AY208893	uec cs618-07 HM369568 (heterotroph cells)
	2	***0***	***0***	***0***	***6***	***6***	***2***	***4***	***3***	***0***	***23***	TOTAL SYNDINIALES		

BGD
10, 15519–15557, 2013

Table 2. Continued.

OTU (Sva_)	O 0904	O 3004	O 1205	O 2106	G1404	G 1205	G 2506	kG 1604	kG 0605	kG 2106	ALL	CLASSIF	ISOLATE	ENVIRONMENTAL CLONE
G2506-1034	2	6		12	9	2	29	20	6	1	**87**	ALV; Cil	Strombidium cf. Basimorphum FJ480419	umec SGUH1454.FRAG.MO.5m JX841568_ ENPaci
G2506-1033	1			1			25			8	**35**	ALV; Cil	Spirotontonia taiwanica FJ715634	umec CNCIII05_210 HM581712 Centr Arc Oce
G2506-1039				7	1	1	7			1	**17**	ALV; Cil	Amphorellopsis quinquealata JQ924058	uec SCM16C17 AY665055 Sargasso Sea
O2106-0706				2			1				**3**	ALV; Cil	Parastrombidinopsis shimi AJ786648	umec BK436 GU433146 Nsea
kG1604-1272								1		1	**2**	ALV; Cil	Pithites vorax FJ870070	umec. CNCIII05_56 HM581716 CentrArcOce
G2506-0986				1			1				**2**	ALV; Cil	Strombidium sp. SBB99-1 AY14356	umec BK328 GU433133 NSea
	3	***6***	***0***	***23***	***10***	***3***	***63***	***21***	***6***	***11***	***146***	TOTAL CILIOPHORA		
kG2106-0850						1		1		13	**15**	TEL	Telonema subtilis AJ564772	umec ANT-Roth-MECL-90 FJ985908_ WAP Rothera
kG2106-0810				4		3	1	1	2	4	**15**	CHOA	Didymoeca costata EU011923	umec SHAA582 JQ226502 NE subarctic Pacif Ocean
kG2106-0882		2		2			7		1	27	**39**	RHI; Cerc	Cryothecomonas aestivalis AF290539	~
O2106-0601	1	4	1	5	2	1		3	2		**19**	RHI; Cerc	Protaspis sp. CC-2009b FJ824125	umec SA24H12 EF526932 Anoxic Framhaven Fjord
O2106-0732				8		1					**9**	RHI; Cerc	Cercozoa sp. CC-2009a FJ824126	umec ANT-Roth-MECL-73 FJ985906 WAP Rothera
O3004-1393	1	1			1			1			**4**	RHI; Cerc	Ebria tripartita DQ303923	umec NA2_1A2 EF526890 Anoxic fjord
kG1604-1312							1	1			**2**	RHI; Cerc	Thaumatomonadida sp. EF023773	euc B12 dil. FN263035
G1404-1161					3	2					**5**	RHI; Haplo	Bonamia ostreae AF262995	~
	2	***7***	***1***	***15***	***6***	***4***	***8***	***5***	***3***	***27***	***78***	TOTAL CERCOZOA		
O1205-0320		58	132			8	2	1	1		**202**	MET; Maxi	Calanus pacificus L81939	umec NPK57_8 EU371277 Kongsfjorden
O21006-0708	9			26			1				**36**	MET; Maxi	Oithona sp. AC-2010 GU594643	umec CNCIII51_10 HM581760 Centr Arc Ocean
	9	***58***	***132***	***26***	***0***	***8***	***3***	***1***	***1***	***0***	***238***	TOTAL COPEPODS		
kG1604-1262								4			**4**	MET; Ann	Aglaophamus trissophyllus GU179368	~
G1404-1074					3						**3**	MET; Loph	Cephalothrix filiformis JF293054	~
kG1604-1291							1	1			**2**	MET; Cni	Sphaeronectes gracilis AF358070	~
G1205-0247						2					**2**	MET;Loph	Macoma nasuta AM774527	~
	0	***0***	***0***	***0***	***3***	***2***	***1***	***5***	***0***	***0***	***11***	TOTAL OTHER METAZOA		
Singletons	**10**	**2**	**4**	**1**	**10**	**5**	**3**	**9**	**3**	**2**	**49**	TOTAL SINGELTONS		

For each OTU **sample-cl. number** we give the main classification, the distribution of clones over each sequenced sample, the total number of sequences for each OTU, the isolate sequence and environmental clone with highest identity to our OTU.
Abbreviations used in the table. Classification section: HAP: *Haptophyceae*; Phae: *Phaeocystales*; Prym: *Prymnesiales*; STR: *Stramenopiles*; Bacil: *Bacillariophyta*; Med: *Mediophyceae*; Cos: *Coscinodiscophyceae*; Frag: *Fragilariophyceae*; Chry: *Chrysophyceae*; Laby: *Labyrinthulomycetes*; Pelag: *Pelagophyceae*; VIR: *Viridiplantae*; Chlo: *Chlorophyta*; Mam: *Mamiellophyceae*; Pras: *Prasinophyceae*; PICOBI: *Picobiliphytes*; CRYP: *Cryptophyta*; Pyren: *Pyrenomonadales*; ALV: *Alveolata*; Dino: *Dinophyceae*; Gymn: *Gymnodiniales*; Sues: *Suessiales*; Peri: *Peridiniales*; Gony: *Gonyaulacales*; un.: unclassified; Syn: *Syndiniales*; Cil: *Ciliophora*; TEL: *Telonemida*; CHOA: *Choanoflagellida*; RHI: *Rhizaria*; Cerc: *Cercozoa*; MET: *Metazoa*; Maxi: *Maxillopoda*; Ann: *Annelida*; Loph: *Lophotrochozoa*; Cni: *Cnidaria*.
Clone section: umec: uncultivated marine eukaryotic clone, uec: uncultivated eukaryotic clone; pico: picoplankton, EN: East-North; NE: North-East; Paci: Pacific Ocean; Centr Arc Oce: Central Arctic Ocean; NSea: North Sea; EAnt: Eastern Antarctic, WAP: Western Antarctic Peninsula.

BGD
10, 15519–15557, 2013

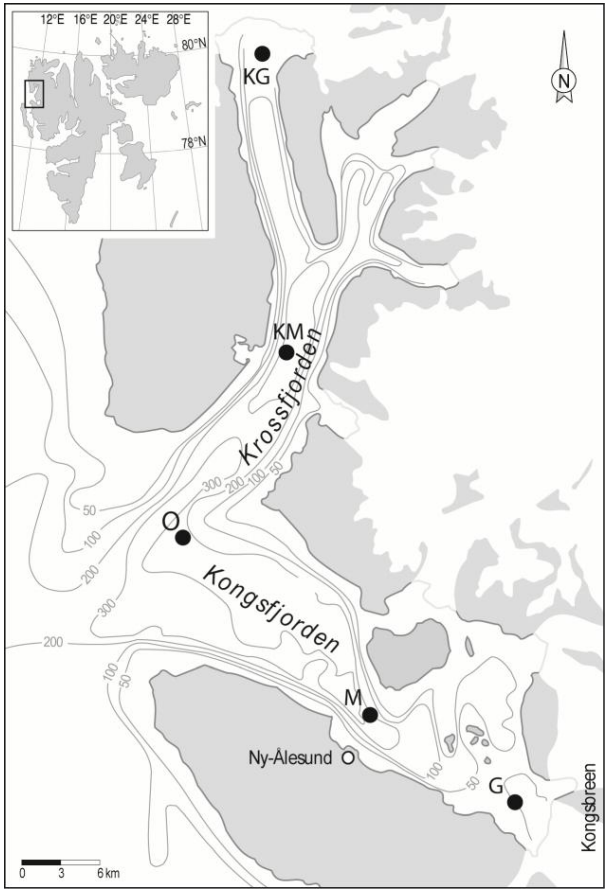

Fig. 1. Bathymetric map of the Kongsfjorden – Krossfjorden system, and inlay map of Svalbard showing the location of the fjords. Sampling locations Ocean (O), Kongsfjorden Middle and Glacier (M and G), Krossfjorden Middle and Glacier stations (KM and KG) are shown on the map.

BGD
10, 15519–15557, 2013

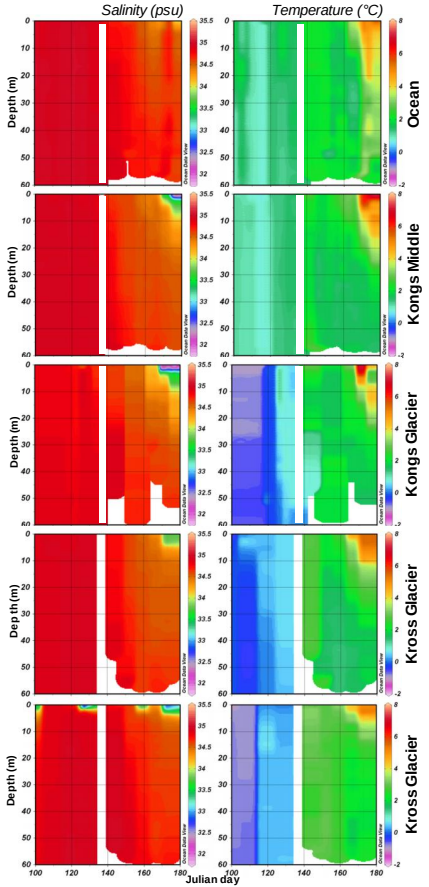

Fig. 2. Water salinity and temperature profiles of the upper 60 m, and of the five sampling stations collected over time in Julian Days (jd.100 is 9 April, and 177 is 25 June. The 2008 (left panel) and 2007 (right panel) sampling periods are separated by a white section.

BGD
10, 15519–15557, 2013

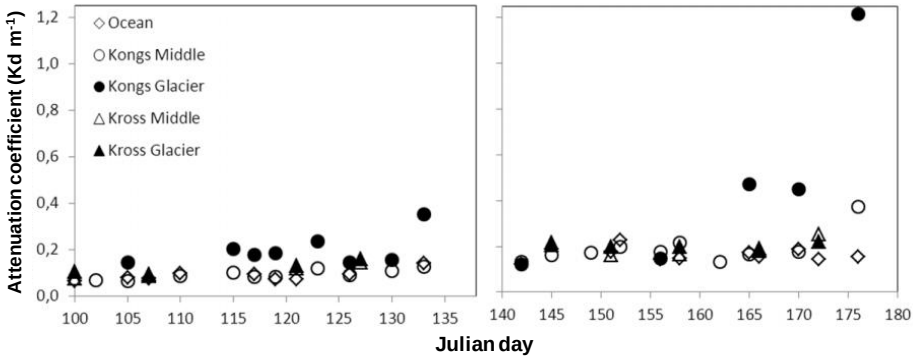

Fig. 3. Change in light attenuation coefficients over time (Julian days) for the 5 stations. Kongs = Kongsfjorden; Kross = Krossfjorden. Left panel: 2008 campaign; right panel: 2007 campaign.

BGD
10, 15519–15557, 2013

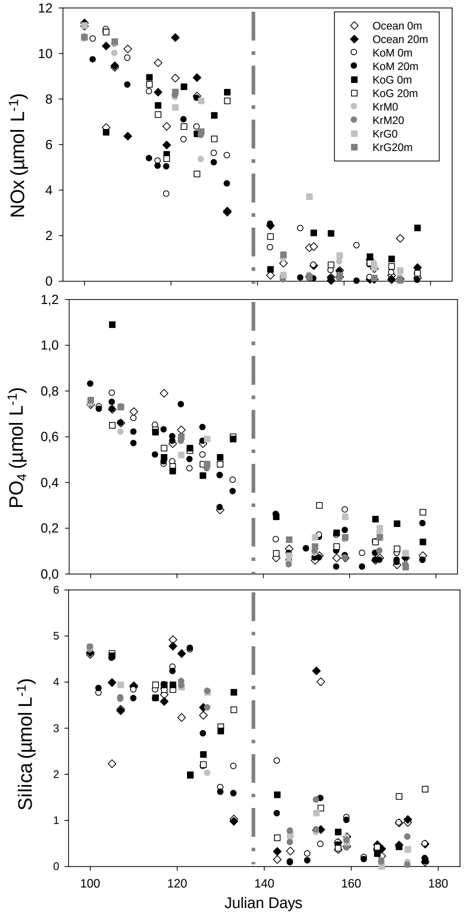

Fig. 4. Nitrate, phosphate and silica concentrations from the five sampling locations collected over time in Julian days. The dotted line separates the 2008 (left panel) from the 2007 (right panel) sampling period.

BGD
10, 15519–15557, 2013

Springtime phytoplankton dynamics

A. M.-T. Piquet et al.

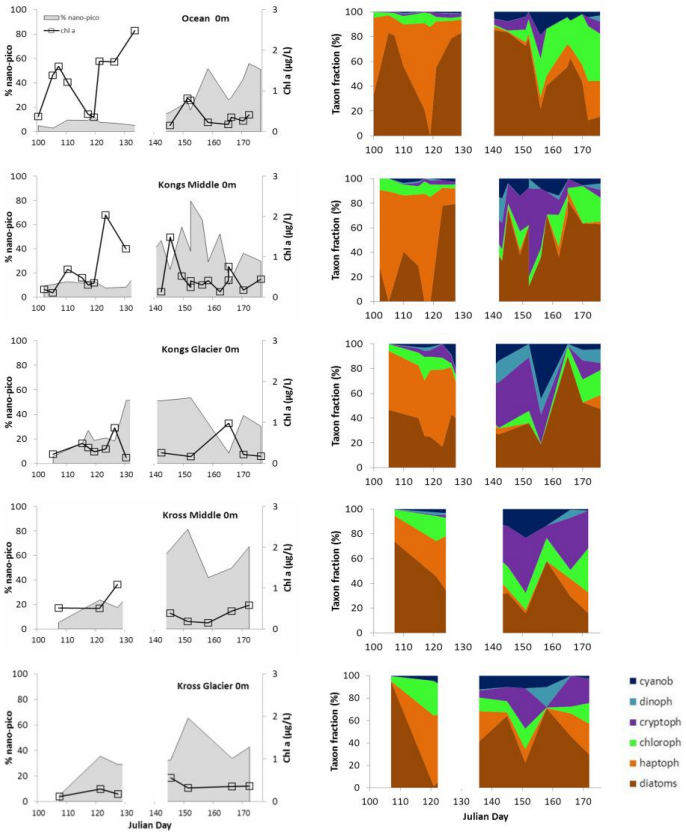

Fig. 5. Surface samples pigment data of all stations over time (Julian days). Left panel show surface biomass (black line) and the relative contribution of nano-picoplankton to the total chl *a* (grey surface). Right panel show the relative pigment class composition (Cyanobacteria, Dinoflagellates, Cryptophytes, Chlorophytes, Haptophytes and Diatoms) to the total chl *a*.

BGD
10, 15519–15557, 2013

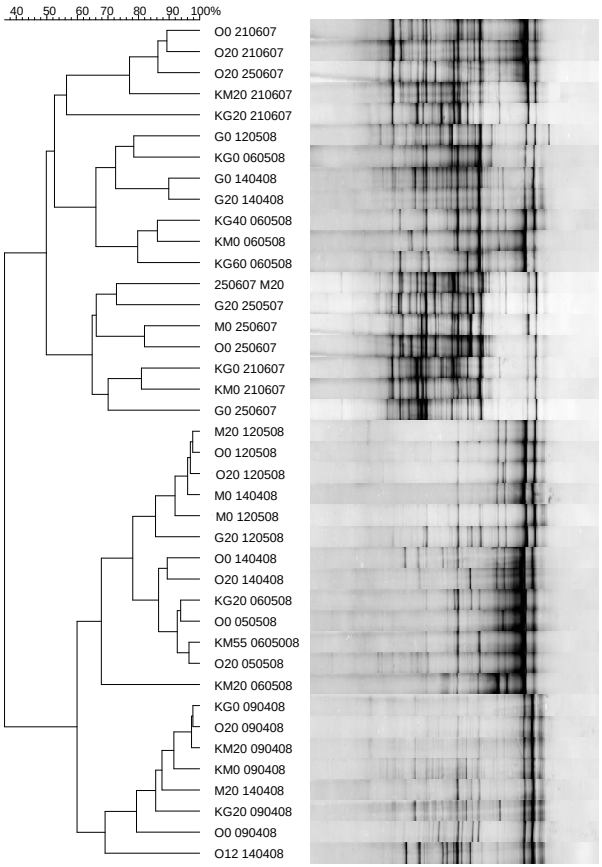

Fig. 6. Dendrogram of DGGE profiles of PCR-amplified 18S rRNA gene fragments from temporal selection of the five sampling locations. The samples were selected according to the maximal temporal range covered by the two field campaigns (early April, early May and end of June). Cluster analysis was based in Pearson's correlation index and the unweighted pair-group method with arithmetic averages.

BGD
10, 15519–15557, 2013